Curved Fatigue Cracks Under Complex Loading

A.C.O. Miranda
L. F. Martha
Department of Civil Engineering, Pontifical Catholic University of Rio de Janeiro (PUC-Rio)

M.A. Meggiolaro
J.T.P. Castro
Department of Mechanical Engineering, Pontifical Catholic University of Rio de Janeiro (PUC-Rio)

T.N. Bittencourt
Department of Structures and Foundations Engineering, Polytechnic School at the University of São Paulo

ABSTRACT

A reliable and cost effective two-phase methodology is proposed to predict crack propagation life in generic two-dimensional structural components under complex fatigue loading. First, the usually curved fatigue crack path and its stress intensity factors are calculated at small crack increments in a specialized finite element software, using automatic remeshing algorithms, special crack tip elements and appropriate crack increment criteria. Then, the calculated stress intensity factors are transferred to a powerful general purpose fatigue design software based in the local approach, which has been designed to predict both initiation and propagation fatigue lives by all classical design methods. In particular, its crack propagation module accepts any $\mathbf{K_I}$ expression and any **da/dN** rule, considering sequence effects such as overload-induced crack retardation to deal with one and two-dimensional crack propagation under complex loading. Non-trivial application examples compare the numerical simulation results with those measured in physical experiments.

INTRODUCTION

The prediction of the fatigue crack propagation life under complex loading in intricate two-dimensional (2D) structural components is a challenging problem, that can be optimally solved by mixing the so-called global and local design approaches.

The crack path (that is generally curved in complicated structures) and its associated stress intensity factors $\mathbf{K_I}$ and $\mathbf{K_{II}}$ can be conveniently calculated by a finite element (FE) global discretization of the component, using appropriate crack tip elements, mesh regeneration schemes and crack increment criteria. However, this approach is not computationally efficient when the load is complex, since it requires remeshing procedures and FE recalculations of the stress/strain field of the whole structure at each load event. Both tasks demand intensive and time-consuming numerical calculations. Moreover, the modeling of crack retardation effects increase the numerical burden and compromise even more the global approach efficiency.

On the other hand, the local approach can be efficiently used to calculate the crack increment at each load cycle, considering crack retardation effects if necessary. This method is based on the direct integration of the material crack propagation rule, using the stress intensity expression for the crack. However, $\mathbf{K_I}$ solutions are simply not available for most real components, and the errors involved in using handbook expressions as an approximation increase as the real crack deviates from the tabulated one, making the local approach accuracy questionable and its predictions unreliable in those cases.

Since the advantages of the global and the local approaches are complementary, the crack propagation problem can be successfully divided in two steps. First, the crack path and its associated mode I stress intensity factor $\mathbf{K_I(a)}$ along the crack length **a** are calculated, under ***simple*** loading, at small discrete steps using an appropriate FE software. Then, an analytical expression is adjusted to the discrete $\mathbf{K_I(a)}$ calculated values, and exported to a local approach software. Finally, the actual ***complex*** loading is efficiently treated by the integration of the crack propagation rule, considering retardation effects if required.

The purpose of this paper is to describe the fundamentals of such an integrated system composed of two complementary programs, designed and tested to implement this two-step hybrid method. This system demonstrates that satisfactory fatigue life predictions under complex load for arbitrary 2D structural components can now be obtained even in PC environments. The next section describes the numerical procedures to compute stress intensity factors in 2D geometries.

NUMERICAL COMPUTATION OF STRESS-INTENSITY FACTORS

In 2D finite element models, three methods can be chosen to compute the stress-intensity factors along the (generally curved) crack path:

(i) the Displacement Correlation Technique (**DCT**) [1];

(ii) the potential energy release rate computed by means of a Modified Crack-Closure (**MCC**) integral technique [2,3]; and

(iii) the **J**-integral computed by means of the Equivalent Domain Integral (**EDI**) together with a mode decomposition scheme [4,5].

Since Bittencourt et al. [6] showed that for sufficiently refined FE meshes all three methods predict essentially the same results, only the DCT method is presented here. The other two methods provide good results even for relatively coarse meshes and should be used preferentialy. Further details can be found in Miranda et al. [7].

In the DCT method, the displacements obtained from the finite element analysis at specific locations are correlated with the analytic solutions expressed in terms of the stress-intensity factors. For quarter-point singular elements [1], the crack opening displacement δ is given by:

$$\delta(r) = (4v_{j-1} - v_{j-2})\sqrt{\frac{r}{L}} = K_I\left(\frac{\kappa+1}{\mu}\right)\sqrt{\frac{r}{2\pi}} \qquad (1)$$

where v_{j-1} and v_{j-2} are the relative displacements in the **y** direction at the **j-1** and **j-2** nodes (see Figure 1), **L** is the element size, $\kappa = 3 - 4\nu$ in plane strain, $\kappa = (3 - \nu)/(1 + \nu)$ in plane stress, ν is the Poisson ratio, and μ is the shear modulus. From Eq. (1), the Mode I (and analogously the Mode II) stress-intensity factor can be evaluated by:

$$K_I = \left(\frac{\mu}{\kappa+1}\right)\sqrt{\frac{2\pi}{L}}(4v_{j-1} - v_{j-2})$$
$$K_{II} = \left(\frac{\mu}{\kappa+1}\right)\sqrt{\frac{2\pi}{L}}(4u_{j-1} - u_{j-2}) \qquad (2)$$

where u_{j-1} and u_{j-2} are the relative displacements in the **x** direction at the **j-1** and **j-2** nodes near the crack tip, see Figure 1.

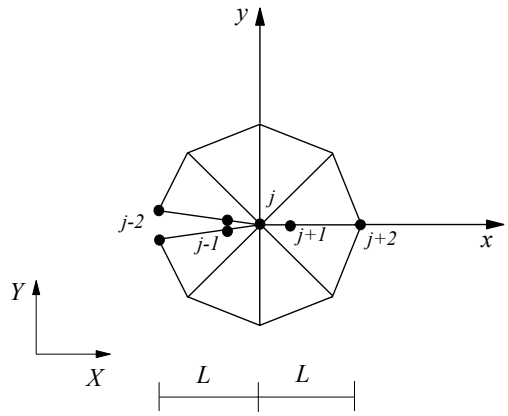

Figure 1. Quarter-point elements at the crack tip.

NUMERICAL COMPUTATION OF THE CRACK INCREMENT DIRECTION

Fatigue cracks almost always propagate in mode I, curving their paths if necessary to avoid rubbing their faces. To simulate this behavior in 2D finite element analysis, the three most used criteria for numerical computation of crack growth in the linear-elastic regime are: (i) the Maximum Circumferential Stress ($\sigma_{\theta max}$); (ii) the Maximum Potential Energy Release Rate ($G_{\theta max}$); and (iii) the Minimum Strain Energy Density ($S_{\theta min}$).

In the first criterion, Erdogan and Sih [8] considered that the crack extension should occur in the direction that maximizes the circumferential stress in the region close to the crack tip. In the second, Hussain et al. [9] have suggested that the crack extension occurs in the direction that causes the maximum fracturing energy release rate. And in the last criterion, Sih [10] assumed that the crack growth direction is determined by the minimum strain energy density value near the crack tip. Bittencourt et al. [6] have shown that if the crack orientation is allowed to change in automatic fracture simulation, the three criteria furnish basically the same numerical results. Since the Maximum Circumferential Stress criterion is the simplest, even presenting a closed form solution, it is the criterion described below.

The stresses at the crack tip for Modes I and II are given by summing up the stress fields generated by each mode:

$$\sigma_r = \frac{1}{\sqrt{2\pi r}}\cos\left(\frac{\theta}{2}\right)\left\{K_I\left[1+\sin^2\left(\frac{\theta}{2}\right)\right]+\frac{3}{2}K_{II}\sin\theta-2K_{II}\tan\left(\frac{\theta}{2}\right)\right\} \quad (3)$$

$$\sigma_\theta = \frac{1}{\sqrt{2\pi r}}\cos(\theta/2)\left[K_I\cos^2(\theta/2)-\frac{3}{2}K_{II}\sin\theta\right] \quad (4)$$

$$\tau_{r\theta} = \frac{1}{\sqrt{2\pi r}}\cos(\theta/2)\left[K_I\sin\theta+K_{II}(3\cos\theta-1)\right] \quad (5)$$

where σ_r is the normal stress component in the radial direction, σ_θ is the normal stress component in the tangential direction, and $\tau_{r\theta}$ is the shear stress component.These expressions are valid both for plane stress and plane strain. The Maximum Circumferential Stress criterion assumes that crack extension begins on a plane perpendicular to the direction in which σ_θ is maximum (and thus $\tau_{r\theta} = 0$). Monotonic extension shall occur when $\sigma_{\theta max}$ reaches a critical value corresponding to a property of the material (K_{IC} for Mode I). Using $\tau_{r\theta} = 0$, Eqs. (4-5) have a trivial solution $\theta = \pm\pi$ for $\cos(\theta/2) = 0$, and a non-trivial solution otherwise:

$$K_I \sin\theta + K_{II}(3\cos\theta - 1) = 0 \quad (6)$$

Analyzing Eq. (6) for pure Mode I, it is found that $K_{II} = 0$, $K_I\sin\theta = 0$ and $\theta = 0^o$, and for pure Mode II that $K_I = 0$, $K_{II}(3\cos\theta - 1) = 0$ and $\theta = \pm 70.5^o$. These are the extreme θ values of the crack propagation angles. The mixed mode intermediary values are found by solving Eq. (6) for θ, resulting in:

$$\theta = 2\arctan\left(\frac{1}{4}\frac{K_I}{K_{II}} \pm \frac{1}{4}\sqrt{\left(\frac{K_I}{K_{II}}\right)^2 + 8}\right) \quad (7)$$

where the sign of θ is the opposite of the sign of K_{II}.

The computational models described above have been implemented in a software called **Quebra2D** (meaning 2D fracture in Portuguese) [10, 11], an interactive graphics software for simulating two-dimensional fracture processes. This software use a finite element automatic mesh generation algorithm devised specifically for this software [12].

The mesh generation algorithm may be optionally used in an adaptive mesh generation scheme that is based on an *a priori* boundary refinement, such as the scheme devised by Paulino et al. [13]. In this case, the adaptive process first requires the analysis results from an initial finite element mesh, usually rough, with the geometric descriptions, boundary conditions, and their attributes. Then a discretization of the domain's region boundary is performed, based on the geometric properties and on the characteristic sizes of the boundary elements (adjacent to the boundary curves), determined from the error estimate from the previous step of the finite element analysis. From this discretization, a new mesh is generated using the algorithm described above with one minor improvement: as the quadtree structure is used to guide the size of the generated elements, an additional quadtree refinement is performed after the initial quadtree is generated. This additional refinement takes into account the characteristic element sizes that are determined by the error estimation analysis.

THE MODELING OF FATIGUE CRACK GROWTH UNDER COMPLEX LOADING BY THE LOCAL APPROACH

The modeling and calculation automation of the LEFM mode I fatigue crack propagation under complex loading by the *local* approach are discussed below. The loading complexity, whose amplitude can randomly vary in time, is unlimited. Sequence effects, such as overload-induced crack retardation or arrest are also considered. Only mode I is discussed, since fatigue cracks almost always propagate perpendicular to the maximum tensile stress.

The local approach is so called because it does *not* require the global solution of the whole structure's stress field. It is based on the direct integration of the fatigue crack propagation rule of the material, $da/dN = F(\Delta K, R, \Delta K_{th}, K_C, ...)$, where ΔK is the stress intensity range of the propagating crack, $R = K_{min}/K_{max}$ is a measure of the mean load, ΔK_{th} is the fatigue crack propagation threshold, and K_C is the fracture toughness. Therefore, neither the ΔK expression nor the crack propagation rule should have their accuracy compromised in name of mathematical simplicity when using this approach.

Most environmental effects can be dealt with an appropriate **da/dN** rule. However, multiple origins loading which induce stresses whose principal directions vary significantly in time are considered beyond the scope of this discussion.

In the sequence, first the main features of the software **ViDa** (which means life in Portuguese, but also stands for Visual Damagemeter) are concisely described. This software has been developed to automate all the traditional local approach methods used in fatigue design [14, 15], including the **SN**, the **IIW** (for welded structures) and the **εN** for crack initiation, and the **da/dN** for crack propagation. Then the cycle-by-cycle method and the modeling of load sequence effects are discussed.

THE **ViDa** SOFTWARE - The objective of this software is to automate in a friendly environment all the calculations required to predict fatigue life under complex loading by the local approach. It runs on PCs under Windows 95/NT or better operating system, including all the necessary tools to perform the predictions, such as: intuitive and friendly graphical interfaces in six idioms; intelligent

databases for stress concentration and intensity factors, crack propagation rules, material properties and the like; traditional and sequential rain-flow counters; graphic output for all calculated results, including elastic-plastic hysteresis loops and of 2D crack fronts; automatic adjustment of crack initiation and propagation experimental data; an equation interpreter, etc. The crack growth can be calculated considering any propagation rule and any **ΔK** expression that can be typed in (making it an ideal companion to the **Quebra2D** software, which can be used to generate the **ΔK(a)** expression if it is not available in its database).

The software has safety features for automatically stopping the calculations if during any loading event it detects that: (i) $\mathbf{K_{max} = K_C}$; (ii) the crack reaches its maximum specified size; (iii) the stress in the residual ligament reaches the rupture strength of the material $\mathbf{S_U}$; (iv) **da/dN** reaches **0.1mm/cycle** (above this rate the problem is fracturing, not fatigue cracking); or else if (v) one of the borders of the piece is reached by the crack front, in the 2D crack propagation case (however, for some geometries the software is able to model the transition from 2D part-through to 1D through cracks). Moreover, it informs when there is yielding in the residual ligament before the maximum specified crack size or number of load cycles is reached. In this way, the calculated values can be used with the guarantee that the limit of validity of the mathematical models is never exceeded.

CYCLE-BY-CYCLE INTEGRATION METHOD - The basic idea of this method is to associate to each load reversion the growth that the crack would have if that **1/2** cycle was the only one to load the piece. Using this assumption, it is easy to write a general expression for the cycle-by-cycle crack growth, by any crack propagation rule: if $\mathbf{da/dN = F(\Delta K, R, \Delta K_{th}, K_C,...)}$, and if in the **i**-th **1/2** cycle of the loading the length of the crack is $\mathbf{a_i}$, the stress range is $\mathbf{\Delta\sigma_i}$ and the mean load causes $\mathbf{R_i}$, then the crack grows by a $\mathbf{\delta a_i}$ given by:

$$\delta a_i = \frac{1}{2} \cdot F(\Delta K(\Delta\sigma_i, a_i), R(\Delta\sigma_i, \sigma_{max_i}), \Delta K_{th}, K_c ...) \qquad (8)$$

The total growth of the crack is quantified by $\mathbf{\Sigma(\delta a_i)}$. Therefore, the cycle-by-cycle rule is similar in concept to the linear damage accumulation used in the **SN** and **εN** fatigue design methods. As in Miner's rule, it requests that *all* the events that cause fatigue damage be recognized before the calculation, e.g. by rain-flow counting the loading. But since it must be applied sequentially, it can be used recognize load interaction effects.

The traditional rain-flow counting algorithm alters the loading *order*, as shown in Figure 2. This can cause serious problems in the predictions, since the loading order effects in crack propagation are of *two* different natures: (i) *delayed* effects, that can retard or stop the subsequent growth of the crack due, e.g., to plasticity-induced Elber-type crack closure [16] or to crack tip bifurcation (these interaction effects among the loading cycles normally increase the crack life and, if neglected, may induce excessively conservative predictions); and (ii) *instantaneous* fracture, that occurs in the first load peak where $\mathbf{K_{max} \geq K_C}$, an event which must, of course, be precisely predicted.

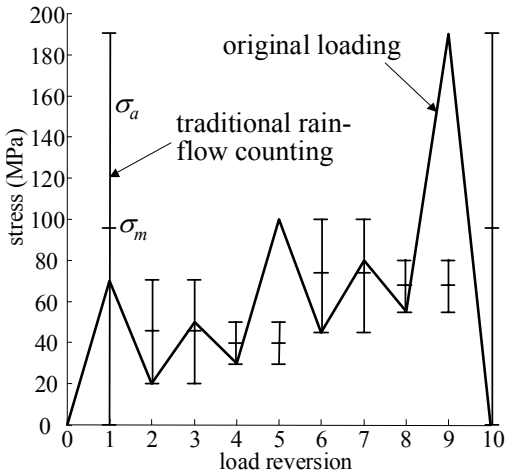

Figure 2. Traditional rain-flow counting (anticipating the large load events).

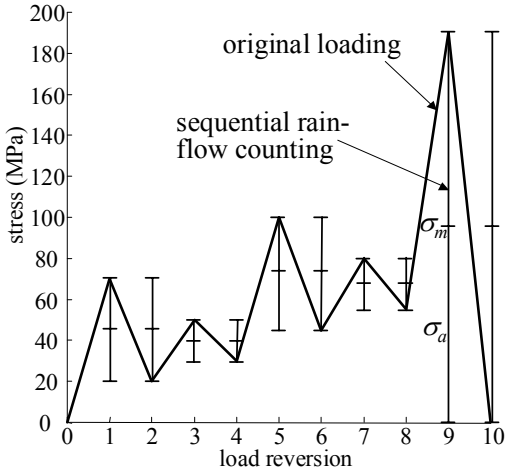

Figure 3. Sequential rain-flow counting (preserving most of the loading order).

Since the **ViDa** loading input can preserve the time *order* information, a *sequential* rain-flow counting option was introduced in that software. With this technique, the effect of each large loading event is counted when it happens (and not *before* its occurrence, as in the traditional rain-flow method), see Figure 3.

The main advantage of the sequential rain-flow counting algorithm is to avoid the premature calculation of the overload effects, which can cause *non*-conservative crack propagation life predictions: as $\mathbf{K(\sigma, a)}$ in general grows

with the crack, a given overload applied when the crack is large can be much more harmful than applied when the crack is small. The sequential rain-flow avoids most sequencing problems caused by the traditional method, and it is certainly an advisable option since it presents advantages over the original algorithm, maintaining its main features without increasing its difficulty.

The computational implementation of Eq. (8) is *not* numerically efficient, even if the compressive peaks and valleys are pre-zeroed and/or the loading is range filtered to eliminate the small events which do not cause fatigue damage. For this reason, an additional feature was introduced to reduce the computational time: an option for maintaining the geometrical part of ΔK constant during small variations in crack size.

As $\Delta K = \Delta\sigma \cdot [\sqrt{(\pi a)} \cdot f(a/W)]$, where $f(a/W)$ is a non-dimensional function (usually quite complex) that depends only on the piece and crack geometry and not on the loading, it can be said that the range of the stress intensity factor ΔK_i at each load reversion depends on two variables of different nature: (i) on the stress range $\Delta\sigma_i$ in that event, and (ii) on the length of the crack a_i in that instant.

$\Delta\sigma_i$, of course, can vary significantly at each event when the loading is complex, but fatigue cracks always grow very slowly. In fact, at least in structural metals, the largest rates of stable crack growth observed in practice are on the order of μm/cycle, and during most of their life the fatigue crack growth rates are better measured in nm/cycle.

Therefore, advantage was taken of the small changes in $f(a/W)$ during small increments in crack length. Instead of calculating $\Delta K_i = \Delta\sigma_i \cdot [\sqrt{(\pi a_i)} \cdot f(a_i/W)]$ at each load cycle, a task that demands great computational effort, a feature was introduced to hold $f(a_i/W)$ constant during a (small) percentage of crack increment $\delta a\%$ (specifiable by the software user depending on the desired precision), an integration method that is numerically much more efficient.

LOAD INTERACTION MODELS - It is well known that load cycle interactions effects can be very important when predicting fatigue crack growth. There is a vast literature proving that tensile overloads can cause retardation or arrest of the subsequent crack growth, and that even compressive underloads can sometimes affect the rate of crack propagation [16, 17, 18].

Neglecting load interaction effects in fatigue life calculations can completely invalidate the predictions. In fact, only after considering overload induced retardation effects can the life reached by real structural components be justified when modeling many practical problems. However, the generation of an universal algorithm to quantify these effects is particularly difficult, due to the number and to the complexity of the mechanisms involved, such as plasticity-induced crack closure, blunting and/or bifurcation of the crack tip, residual stress and/or strain fields, strain-hardening and/or strain-induced fase transformation, crack face roughness, and oxidation of the crack faces, e.g. Besides, depending on the case, several of these mechanisms may act concomitantly or competitively, as a function of factors such as crack size, material microstructure, dominant stress state, and environment.

On the other hand, the principal characteristic of fatigue cracks is to propagate cutting a material that has already been deformed by the plastic zone that always accompanies their tips. The fatigue crack faces are embedded in an envelope of (plastic) residual strains and, consequently they compress their faces when completely discharged, and open alleviating in a progressive way the (compressive) load transmitted through their faces.

According to Elber [19], only after completely opening the crack at a load K_{op}, would the crack tip be stressed. Therefore, the bigger the K_{op}, the less would be the effective stress intensity range $\Delta K_{eff} = K_{max} - K_{op}$, and this ΔK_{eff} instead of ΔK would be the fatigue crack propagation rate controlling parameter. Most load interaction models are, although indirectly, based in this idea. This implicates in the supposition that the principal retardation mechanism is caused by plasticity induced crack closure: in these cases, the opening load should *increase* when the crack penetrates into the plastic zone inflated by the overload, *reducing* the ΔK_{eff} and stopping or delaying the crack, while the plastic zones associated with the loading are contained in the overload induced plastic zone.

Several mathematical models have been developed to account for load interaction in crack propagation based on Elber's crack closure idea. In these methods, the retardation mechanism is only considered within the plastic zone situated in front of the crack tip. According to these procedures, a larger plastic zone Z_{ol} is created by means of an overload, see Figure 4. When the overload is removed, an increased compressive stress state is set up in the volume of its plastic zone, reducing crack propagation under a smaller succeeding load cycle.

The detailed discussion of this complex phenomenology is considered beyond the scope of this work, but a revision of the phenomenological problem can be found in [16]. A taxonomy of the load interaction models has been introduced by Meggiolaro and Castro [18], including proposed modifications to better model such effects as crack arrest, crack acceleration due to compressive underloads, and the effect of small cracks. They classified these models in 4 categories: (i) da/dN models, such as the Wheeler model, which use retardation functions to directly reduce the calculated crack propagation rate da/dN; (ii) ΔK models, such as the Modified Wheeler model, which use retardation functions to reduce the value of the stress intensity

factor range **ΔK**; (iii) $\mathbf{R_{eff}}$ models, such as the Willenborg model, which introduce an effective stress ratio $\mathbf{R_{eff}}$, calculated by reducing the maximum and minimum stress intensity factors acting on the crack tip, however not necessarily changing the value of **ΔK**; and (iv) $\mathbf{K_{op}}$ models, such as the strip yield model, which use estimates of the opening stress intensity factor $\mathbf{K_{op}}$ to directly account for Elber-type crack closure.

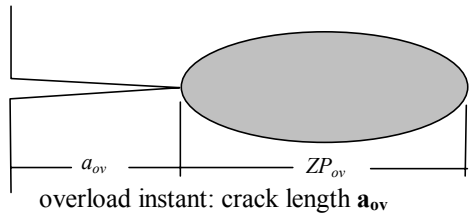

overload instant: crack length $\mathbf{a_{ov}}$

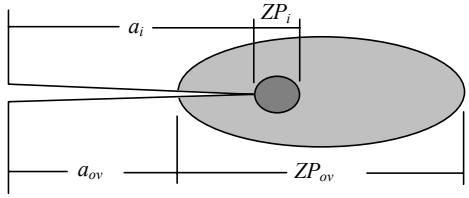

retardation zone: $\mathbf{a_i + ZP_i < a_{ov} + ZP_{ov}}$

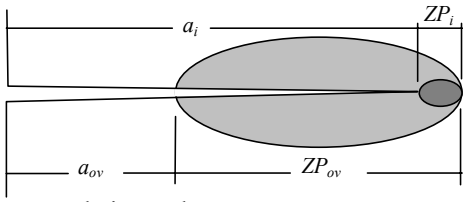

retardation end: $\mathbf{a_j + ZP_j = a_{ov} + ZP_{ov}}$

Figure 4. Yield zone crack growth retardation region used by the Wheeler and Willenborg load interaction models.

There are other retardation models, but none of those that can be implemented in a local approach code has definitive advantages over the models discussed above. This is no surprise, since single equations are too simplistic to model all the several mechanisms that can induce retardation effects. Therefore, in the same way that a curve **da/dN** vs. **ΔK** is experimentally measured, a propagation model should be adjusted to experimental data to calibrate the retardation models, as recommended by Broek [17].

The numerical implementation of these retardation models in a cycle-by-cycle algorithm is not conceptually difficult, but it requires a considerable programming effort [18]. All load interaction models presented in that paper have been implemented in the **ViDa** software.

EXPERIMENTAL VERIFICATION OF THE CRACK PROPAGATION MODELING PROCEDURES IN ARBITRARY 2D GEOMETRIES

This section describes the modeling and testing procedures used for studying the fatigue crack propagation problem in modified four point bending single edge notch (SEN) and compact tension (CT) test specimens, in which holes were machined to curve the crack propagation path, see Figures 5 and 6.

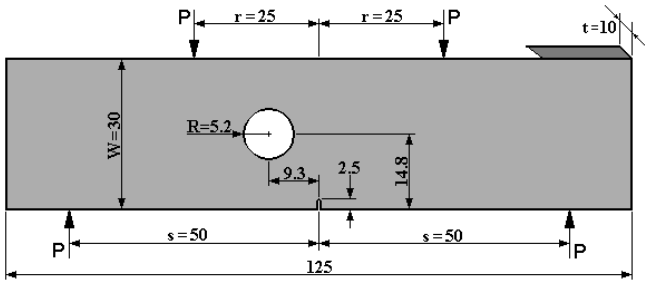

Figure 5 – Details of the modified SEN specimen.

The tested material was a cold rolled SAE 1020 steel, with the analyzed weight per cent composition: C 0.19, Mn 0.46, Si 0.14, Ni 0.052, Cr 0.045, Mo 0.007, Cu 0.11, Nb 0.002, Ti 0.002, Fe balance. **E = 205GPa** was the Young's modulus, $\mathbf{S_Y}$ **= 285MPa** the yield strength, $\mathbf{S_U}$ **= 491MPa** the ultimate strength, and **RA = 53.7%** the area reduction. These properties were measured according to the ASTM E 8M-99 standard. The **da/dN** vs. **ΔK** data, obtained under a stress ratio **R = 0.1** and measured following ASTM E 647-99 procedures, was fitted by the modified Elber equation $\mathbf{da/dN = 4.5 \cdot 10^{-10} \cdot (\Delta K - \Delta K_{th})^{2.05}}$, where the threshold stress intensity range was $\mathbf{\Delta K_{th} = 11.6 MPa\sqrt{m}}$.

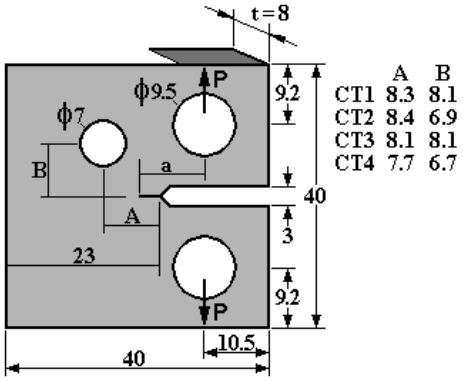

Figure 6 – Details of the modified CT specimens.

Before the tests, the hole-modified SEN and CT specimens were FE modeled following the procedures described above. Then the hole position was varied in the models to obtain the most interesting curved crack path, by a simple trial-and-error process. The chosen specimen geometries were machined, measured and FE remodeled, to account for small deviations in the manufacture. In this way, it could be assured that the numeric models used in the predictions reproduced the real geometry of the tested specimens.

The FE models generated $\mathbf{K_I}$ values computed by the MCC technique at short but discrete intervals along the predicted crack paths, which were calculated by the $\sigma_{\theta max}$

method. The PC used for the numeric procedures was a Pentium 650MHz with 128 Mb of RAM, running under Windows 98 operating system. The FE models were easily created with the friendly interactive graphic facilities of the **Quebra2D** software, where the incremental crack growth simulation is automatic, after specifying its initial size and desired growth step.

Shortly, the automatic calculation procedure was: (i) the FE model of the holed specimen with the specified initial crack was solved to obtain its $\mathbf{K_I}$ and $\mathbf{K_{II}}$ stress-intensity factors and the corresponding propagation direction; (ii) the crack was incremented in the growth direction by the (small) required step; (iii) the model was remeshed to account for the new crack size; and (iv) the process was iterated until the required final crack size was reached.

Each calculation step, including the automatic remeshing and the FE solution for $\mathbf{K_I}$, $\mathbf{K_{II}}$ and the incremental growth direction lasted about four seconds in the used PC. With an average of thirty increments to simulate the whole crack growth, the total calculation process consumed about two minutes. Therefore, it was indeed practical to implement the trial-and-error procedure to optimize the test specimens.

Although the crack path geometry is 2D, once it is known the crack itself can be described by its (one dimensional) length **a** measured along the crack path. Hence, its $\mathbf{K_I}$ can be written as a function of **a**, $\mathbf{K_I(a) = \sigma\sqrt{\pi a}\cdot f(a/w)}$. The discretely calculated values of the geometry factor **f(a/w)** were exported to the **ViDa** software, where they were automatically adjusted by an appropriate continuous analytical function.

Then the load programs that would be applied during the tests were calculated to maintain a quasi-constant stress intensity range around $\mathbf{\Delta K_I \approx 20MPa\sqrt{m}}$, with $\mathbf{R = K_{min}/K_{max} = 0.1}$. These loading values induce a stage II (Paris regime) fatigue crack growth in the 1020 steel **da/dN** vs. $\mathbf{\Delta K}$ curve. The fatigue lives associated with the load programs were predicted in about 3 seconds.

The experimental procedures used during the tests were very similar to those used in the standard measurement of **da/dN** vs. $\mathbf{\Delta K}$ curves. All the tests were run at a 20 Hz frequency in a 250kN computer controlled servo-hydraulic testing machine. The loads were regularly adjusted to maintain the specified quasi-constant $\mathbf{\Delta K_I}$. The only difference was the use of a digital camera and an image analysis program to measure the crack size *and* path. This is a precise and know also quite economical option to automate those measurements, but its details are considered beyond the scope of this paper.

Following the tests, the real crack path was measured and the lives at each load step were compared with the predicted ones. These results are discussed below.

SEN SPECIMEN - A crack was fatigue propagated in a SEN specimen with a hole slightly to the left of the starting notch (created using a 0.3mm jeweler's saw), as shown in Figure 5. The final FE mesh automatically generated for predicting the propagation path is illustrated in Figure 7. Note the density of the mesh around the crack path and, particularly, around its tip. The initial mesh had 1995 elements and 4185 nodes, and the final one 2585 elements and 5467 nodes.

Figure 8 compares the **f(a/w)** expression calculated for this holed test specimen with the standard SEN expression obtained from the literature[17]. It can be observed that the hole has a significant influence in the **f(a/w)** value.

Figure 9 shows a picture of the real crack path after the test and the FE crack path prediction made *before* the test. This modeling has been indeed quite satisfactory. Therefore, the calculated $\mathbf{K_I}$ values could also be used to check the predicted fatigue life.

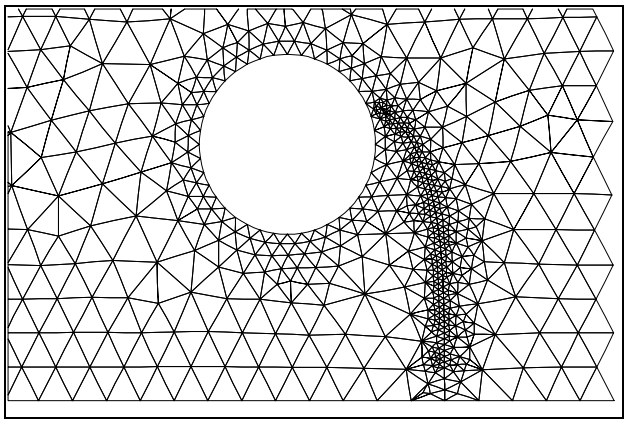

Figure 7 – FE mesh automatically generated for the modified SEN specimen.

However, a significant deviation was observed when comparing the experimental data with the predicted life. They only agreed during part of test, as shown in Figure 10. But after about 440,000 load cycles, a clear deviation was present in the **a** vs. **N** graph. The initial agreement indicated that the predicted $\mathbf{K_I}$ were reproducing the expected crack growth rate, a renewed indication that the modeling was obtaining satisfactory results. As the modeling was constant, it was concluded that an unplanned accident occurred during the test.

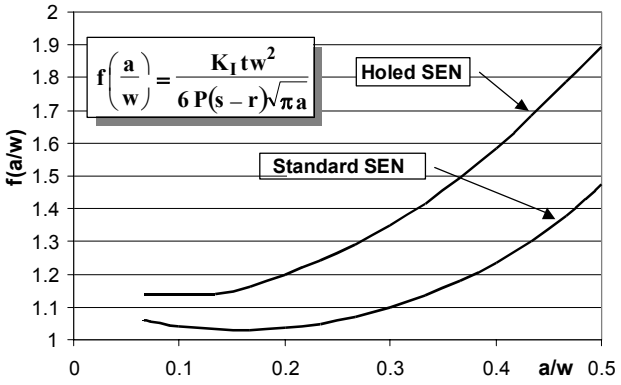

Figure 8 – **f(a/w)** expression for the modified SEN specimen.

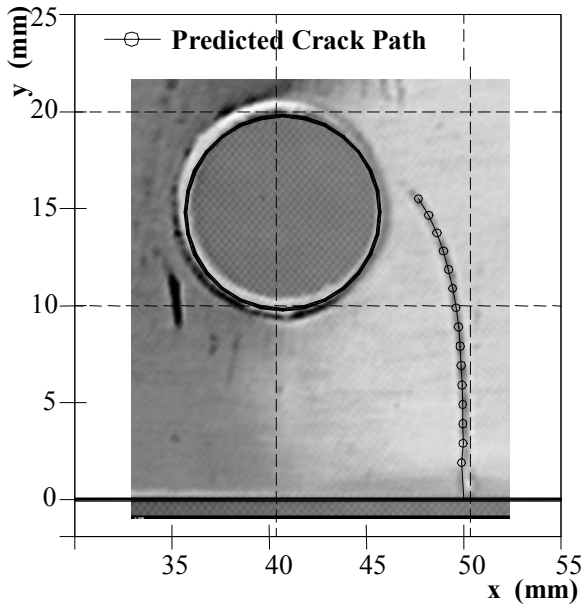

Figure 9 – The real and the predicted crack paths for the modified SEN specimen.

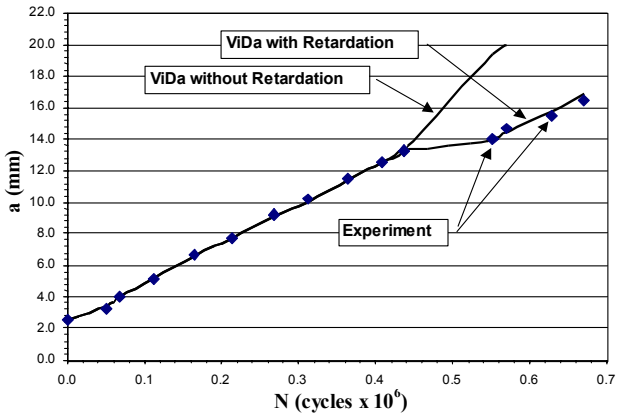

Figure 10 – Predicted and measured fatigue crack propagation behavior for the modified SEN specimen.

Indeed, a review of the loading history identified that an accidental **60%** overload had occurred at around 440k cycles during a load adjustment procedure, and this was confirmed by a larger plastic zone observed on the crack path at that point. This single overload was then simulated on the ViDa software, using its retardation modeling facilities. The Modified Wheeler model, which has quite interesting features as discussed by Meggiolaro & Castro [18], was used with an exponent γ = **1.43** to simulate this crack growth retardation problem. The simulation satisfactorily reproduced the whole crack growth behavior observed during the test of the holed SEN, as also shown in Figure 10.

CT SPECIMEN - Four modified CT specimens were tested. Each one had a **7mm** diameter hole positioned at a horizontal **A** and a vertical **B** distance from the notch root, as shown in Figure 6. This odd configuration was chosen because two different crack growth behaviors were predicted by the FE modeling the holed specimen, depending on the hole position. The fatigue crack was always attracted by the hole, but it could grow toward it or just be deflected, missing the hole and continuing to propagate after passing it. Figure 11 illustrates these predicted crack paths. The initial meshes in the FE models had about 1300 elements and 2300 nodes, and the final ones after the simulated crack propagation had about 2200 elements and 5500 nodes. The calculated $\mathbf{K_I}$ values are presented and compared to the standard CTS values in Figure 12.

To test the accuracy of the FE modeling, the transition point between the "sink in the hole" and the "miss the hole" crack growth behaviors was identified. Then, two borderline specimens were dimensioned: one with the hole just half a millimeter below that point and the other with the hole half a millimeter above it. Due to machining tolerances, the actual difference between the holes vertical position in specimens CT1 and CT2 turn out to be 1.2mm instead. These specimens were remodeled to predict the actual crack path. The measured and the predicted crack paths are compared in Fig. 13.

This result was so encouraging that two other specimens, CT3 and CT4, were built to check it. This time, the vertical distance between their holes was 1.4mm, and they were also FE remodeled to account for this deviation. However, the crack path in these specimens were not as well predicted as they were in CT1 and CT2, as shown in Figure 13. The predicted paths in fact were in between the measured ones in the two faces of the specimens, and this was an indication that an unwanted transversal moment had also loaded them. Indeed, after the latter tests frictional problems were found in the universal joint of the load train, which had to be substituted. But these not so good results are presented here to illustrate the mean path FE prediction. The predicted and measured fatigue lives are shown in Figures 14 to 17.

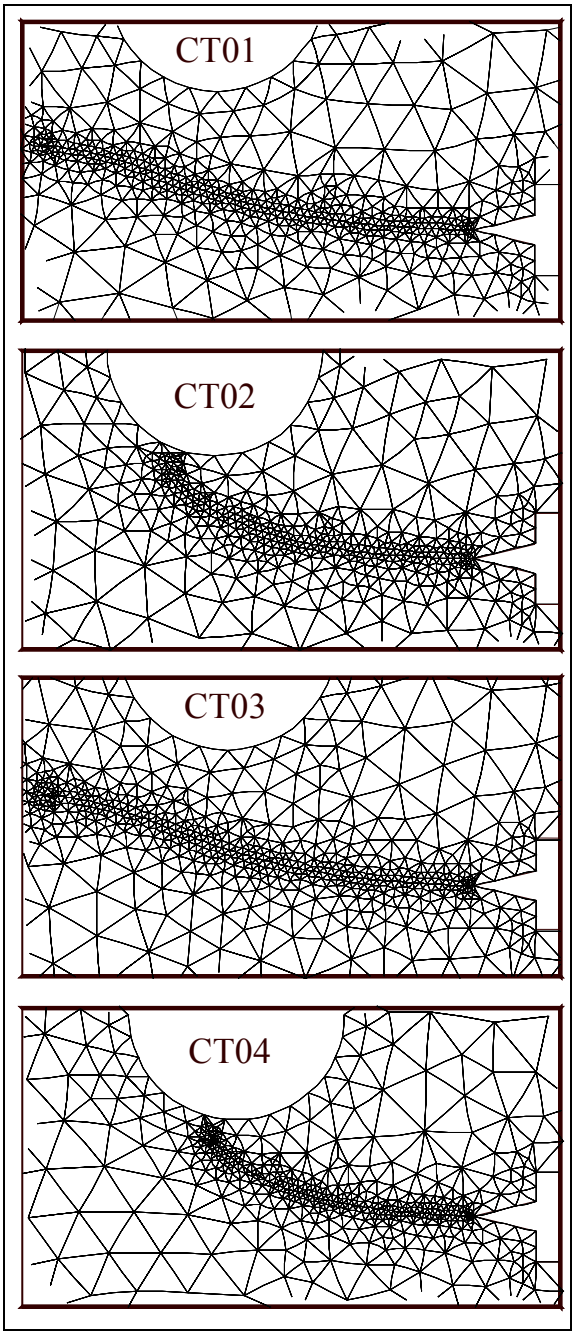

Figure 11 – FE mesh automatically generated for the modified CT specimens.

CONCLUSIONS

A two-phase methodology was presented to predict fatigue crack propagation in generic 2D structures under complex loading. First, self-adaptive finite elements were used to calculate, by three different methods, the fatigue crack path and the stress intensity factors along the crack length $\mathbf{K_I(a)}$ and $\mathbf{K_{II}(a)}$, at each propagation step. The calculated $\mathbf{K_I(a)}$ was then used to predict the propagation fatigue life by the local approach, using the cycle-by-cycle integration methods considering overload-induced crack retardation effects. Two complementary software were developed to implement this methodology. The first one is an interactive graphical program for simulating two-dimensional fracture processes based on a finite element adaptive mesh generation strategy. The second is a general purpose fatigue design software developed to predict both initiation and propagation fatigue lives under complex loading by all classical design methods. In particular, its crack propagation module accepts any stress intensity factor expression, including the ones generated by the finite element software. Experimental results showed that the presented methodology and its software implementation could effectively predict the crack propagation paths and the fatigue lives of arbitrary two-dimensional structural components.

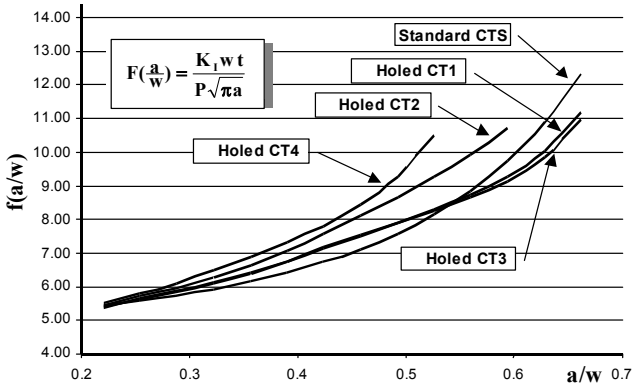

Figure 12 – **f(a/w)** curves for the standard and for the modified CT specimens.

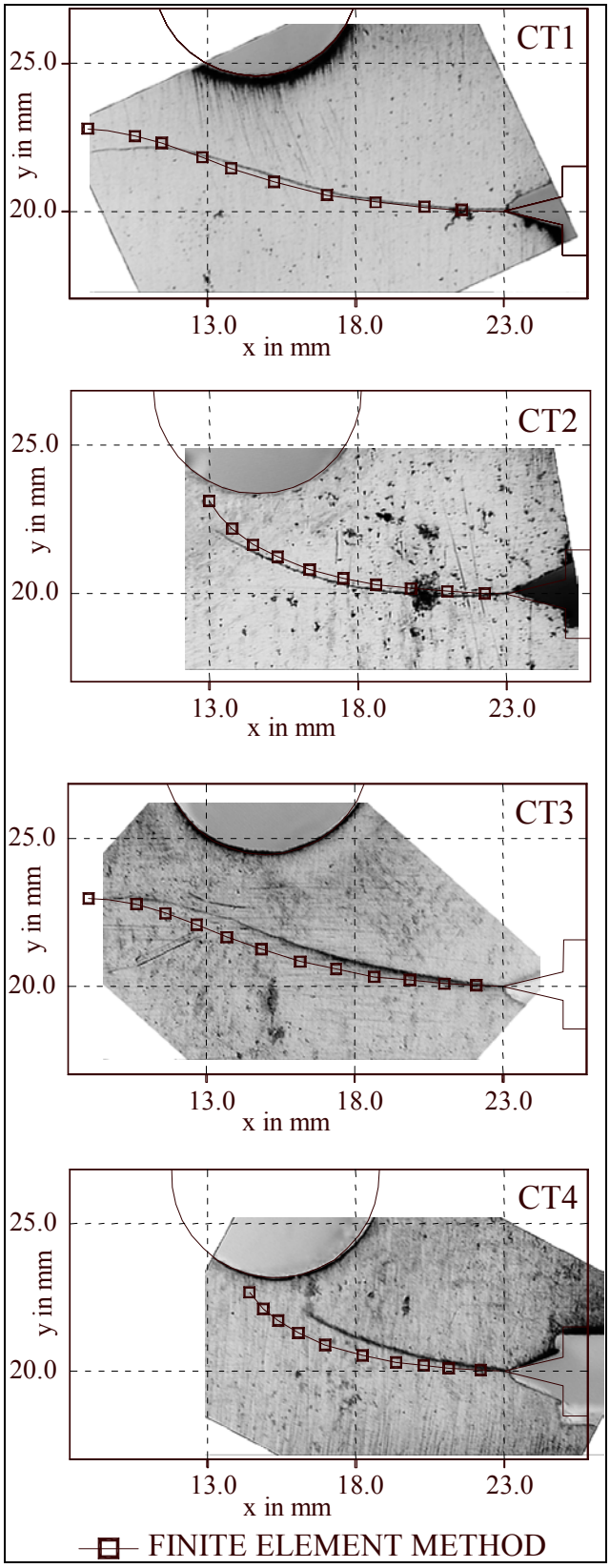

Figure 13 – Predicted and measured crack paths for the modified CT specimens.

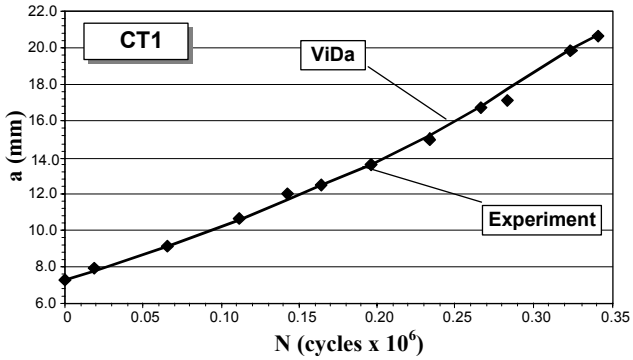

Figure 14 – Predicted and measured fatigue life for CT2.

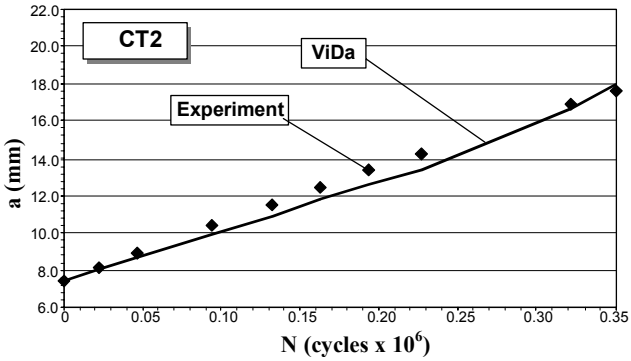

Figure 15 – Predicted and measured fatigue life for CT2.

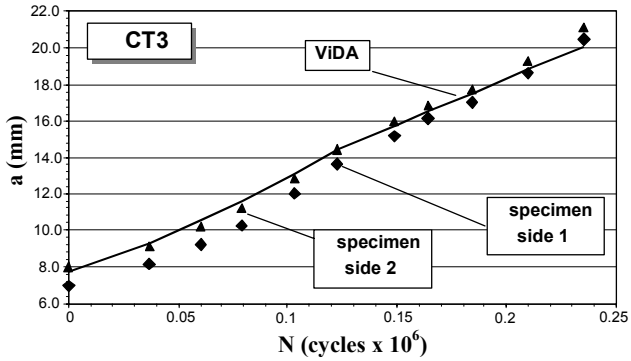

Figure 16 – Predicted and measured fatigue life for CT3.

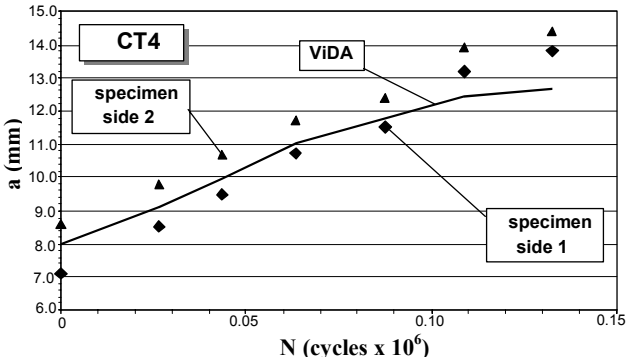

Figure 17– Predicted and measured fatigue life for CT4.

REFERENCES

[1] Shih, C.F., de Lorenzi, H.G., German, M.D. (1976). "Crack Extension Modeling with Singular Quadratic Isoparametric Elements," International Journal of Fracture, **12**, 647-651.

[2] Rybicki, E.F., Kanninen, M.F. (1977). "A Finite Element Calculation of Stress-Intensity Factors by a Modified Crack Closure Integral," Engineering Fracture Mechanics, **9**, 931-938.

[3] Raju, I.S. (1987). "Calculation of Strain-Energy Release Rates with Higher Order and Singular Finite Elements," Engineering Fracture Mechanics, **28**, 251-274.

[4] Nikishkov, G.P., Atluri,S.N. (1987). "Calculation of Fracture Mechanics Parameters for an Arbitrary Three-Dimensional Crack by the Equivalent Domain Integral Method," International Journal for Numerical Methods in Engineering, **24**, 1801-1821.

[5] Dodds, R.H. Jr., Vargas, P.M. (1988). "Numerical Evaluation of Domain and Contour Integrals for Nonlinear Fracture Mechanics," Report, Dept. of Civil Engineering, U. of Illinois, Urbana-Champaign.

[6] Bittencourt, T.N., Wawrzynek, P.A., Ingraffea, A.R., Sousa, J.L.A. (1996). "Quasi-Automatic Simulation of Crack Propagation for 2D LEFM Problems," Engineering Fracture Mechanics, **55**, 321-334.

[7] Miranda, A. C. O., Meggiolaro, M. A., Castro, J. T. P., Martha, L. F. and Bittencourt, T. N., "Fatigue Crack Propagation under Complex Loading in Arbitrary 2D Geometries," Applications of Automation Technology in Fatigue and Fracture Testing and Analysis*, ASTM STP 1411*, A. A. Braun et al., Eds., ASTM, 2002.

[8] Erdogan, F., Sih, G.C. (1963). "On the Crack Extension in Plates under Plane Loading and Transverse Shear," Journal of Basic Engineering, **85**, 519-527.

[9] Sih, G.C. (1974). "Strain-Energy-Density Factor Applied to Mixed Mode Crack Problems," International Journal of Fracture Mechanics, **10**, 305-321.

[10] Araújo, T.D.P., Cavalcante, J.B., Carvalho, M.T.M., Bittencourt, T.N., Martha, L.F. (1997). "Adaptive Simulation of Fracture Processes Based on Spatial Enumeration Techniques," International Journal of Rock Mechanics and Mining Sciences, **34**, 551.

[11] Carvalho, C.V.A., Araújo, T.D.P., Cavalcante Neto, J.B., Martha, L.F., Bittencourt, T.N. (1999). "Automatic Fatigue Crack Propagation using a Self-adaptive Strategy," PACAM VI - Sixth Pan-American Congress of Applied Mechanics, Rio de Janeiro, **6**, 377-380.

[12] Miranda, A.C.O., Cavalcante Neto, J.B., Martha, L.F. (1999). "An Algorithm for Two-dimensional Mesh Generation for Arbitrary Regions with Cracks," Proceedings of XII Brazilian Symposium on Computer Graphics, Image Processing and Vision, UNICAMP/SBC, Campinas, Brazil, Out. 1999, IEEE Computer Society Order Number PRO0481, ISBN 0-7695-0481-7, Eds.: J. Stolfi & C. Tozzi, 29-38.

[13] Paulino, G.H., Menezes, I.F.M., Cavalcante Neto, J.B., Martha, L.F. (1999). "A Methodology for Adaptive Finite Element Analysis: Towards an Integrated Computational Environment," Computational Mechanics, **23**, 361-388.

[14] Meggiolaro, M.A., Castro, J.T.P. (1998). "ViDa 98 - a Visual Damagemeter to Automatize the Fatigue Design under Complex Loading," (in Portuguese), Revista Brasileira de Ciências Mecânicas, **20**, 666-685.

[15] Castro, J.T.P., Meggiolaro, M.A. (1999). "Some Comments on the εN Method Automation for Fatigue Dimensioning under Complex Loading," (in Portuguese), Revista Brasileira de Ciências Mecânicas, **21**, pp.294-312.

[16] Suresh, S. (1998). *Fatigue of Materials*, Cambridge.

[17] Broek, D. (1988). *The Practical Use of Fracture Mechanics*, Kluwer.

[18] Meggiolaro, M.A., Castro, J.T.P. (2001). "Comparison of Load Interaction Models in Fatigue Crack Propagation," XVI Congresso Brasileiro de Eng. Mecânica (COBEM), ABCM, Uberlândia, MG.

[19] Elber, W. (1971). "The Significance of Fatigue Crack Closure," ASTM STP 486.